Wind Effects on Dual Probe Heat Pulse Method Measured Soil Thermal Properties

Yujie Sang, Gang Liu*, Robert Horton

Y. J. Sang and G. Liu, Department of Land Utilization Engineering, College of Land Science and Technology, China Agricultural University, Beijing 100193, China; R. Horton, Department of Agronomy, Iowa State University, Ames, IA 50011, USA. *Corresponding author (liug@cau.edu.cn).

Acknowledgements

This work was supported by the Natural Science Foundation of China (Grant No. 41771257) and the National Key Research and Development Program of China (No. 2016YFD0800102).

Core Ideas

- Experiments and numerical simulations indicate consistently that wind affects DPHP measured surface soil thermal properties.
- The DPHP estimated thermal property values have positive correlations with v.
- The ILS-ABC model better estimates c than does the ILS model when $v \leq 3.5$ m s^{-1}.

This article has been accepted for publication and undergone full peer review but has not been through the copyediting, typesetting, pagination and proofreading process, which may lead to differences between this version and the Version of Record. Please cite this article as doi: 10.1002/saj2.20041.

ABSTRACT

When a dual probe heat pulse (DPHP) sensor is installed in soil near the soil-atmosphere interface, the basic assumptions of the infinite line heat source (ILS) model and its improvement, the infinite line heat source model with an adiabatic boundary condition (ILS-ABC), might not be satisfied because of wind. This study aims at exploring the effects of wind on DPHP measurements and comparing the performance of the ILS and ILS-ABC models with different values of wind velocity (v) and burial depth (d). Our study shows that the results of laboratory experiments, COMSOL simulations, and field experiments are consistent with each other. For dry sand with $d \leq 4$ mm, the effects of wind is non-negligible when $v \geq 3.5$ m s^{-1}, and the DPHP method does not provide accurate estimations whether the ILS model or the ILS-ABC model is used. Field experiments are prone to large background temperature fluctuations which can cause the linear de-trend method of Jury and Bellantuoni (1976) to perform poorly. In general, v is less than 2.7 m s^{-1} in field and for $d = 5$ mm the ILS-ABC model provides more accurate estimations with relative error < 15% in thermal conductivity (λ) and relative error < 9% in heat capacity (c).

Abbreviations: c, heat capacity; d, burial depth; DPHP, dual probe heat pulse; DSC, differential scanning calorimeter; h, heat transfer coefficient; ILS, infinite line heat source; ILS-ABC, infinite line heat source with adiabatic boundary condition; Re, Reynolds number;

v, wind velocity; α, thermal diffusivity; λ, thermal conductivity; λ_a, thermal conductivity of air.

INTRODUCTION

Soil thermal properties are important basic soil parameters, and the DPHP method is a potential way to measure soil heat capacity (c) (Campbell et al., 1991), thermal conductivity (λ) and thermal diffusivity (α) (Bristow et al., 1994, 1995). By using DPHP measured λ values and ambient soil temperature profiles, soil heat flux can be determined (Cobos and Baker, 2003; Kettridge and Baird, 2007; Peng et al., 2017). Because of the relationships between soil water content and soil thermal properties (de Vries, 1963; Cosenza et al., 2003; Lu et al., 2014), some researchers have also used the DPHP method to measure soil water content (Kamai et al., 2015). Other researchers have used DPHP method to determine soil water flux (Hopmans et al., 2002), soil water evaporation dynamics (Heitman et al., 2008) and soil bulk density (Lu et al., 2018). In addition, the DPHP method is also used to measure thermal properties of snow (Sturm et al., 2002) and sap flux density (Ren et al., 2017). Thus, the DPHP method is a useful method to measure numerous physical properties simultaneously (He et al., 2018).

The widely used ILS model is based on an assumption that the soil being measured is an infinite, homogeneous and isotropic medium. However, when the DPHP sensor is installed near the soil–atmosphere interface, the assumption cannot be satisfied, because the

difference between thermal conductivities of air (λ_a) and soil is large (Lemmon and Jacobsen, 2004). Philip and Kluitenberg (1999) and Xiao et al. (2015) showed that underestimations in λ and c will occur when a DPHP sensor is installed near the soil–atmosphere interface. Liu et al. (2013b, 2017) simplify the soil–atmosphere interface into an adiabatic boundary condition, that is, $\lambda_a = 0$ in their assumption, and present the ILS–ABC model by the image method (Carslaw and Jaeger, 1959). Zhang et al. (2014) show that the ILS–ABC model can improve the accuracy of DPHP measurements in the field. If DPHP measurements are made near the soil–atmosphere interface (Heitman et al., 2008; Young et al, 2008; Lu et al., 2018), and there is wind, the DPHP system deviates from the assumptions of the ILS–ABC model, because wind affects mass and energy transfer between the soil and the atmosphere (McCafferty et al., 1997; McVicar et al., 2012; Redecker et al., 2015; Poulsen et al., 2018). Although the effects of wind on DPHP measurements might be significant, neither theoretical analyses nor experiments have yet been performed to evaluate wind effects.

In this study, laboratory experiments, COMSOL simulations and field experiments are performed to explore the effects of wind on DPHP measured surface soil thermal properties.

MATERIALS AND METHODS

Theory

The ILS model is a mainstream model for analyzing DPHP data. In this model, soil is assumed to be an infinite, homogeneous and isotropic medium with uniform initial temperature. When an ILS releases a heat pulse of duration t_0, the temperature rise (ΔT) at radial distance r is (de Vries, 1952):

$$\Delta T(r,t) = \frac{q'}{4\pi\lambda}\left\{Ei\left[\frac{-r^2}{4\alpha(t-t_0)}\right] - Ei\left[\frac{-r^2}{4\alpha t}\right]\right\} \quad t \geq t_0 \tag{1}$$

where q' is the energy input per unit length of heater per unit time (W m^{-1}), λ is the thermal conductivity (W m^{-1} K^{-1}), -Ei(-x) is the exponential integral, α is the thermal diffusivity (m^2 s^{-1}), t is the time (s) beginning from a heat pulse initiation.

Liu et al. (2013b, 2017) propose the ILS-ABC model for approximating the soil-atmosphere interface. In their model, the image method (Carslaw and Jaeger, 1959) is used to treat the adiabatic boundary by introducing a virtual heating probe which has reflection symmetry about the soil-atmosphere interface. ΔT for the ILS-ABC model is expressed as:

$$\begin{aligned}\Delta T(r,t) = {} & \frac{q'}{4\pi\lambda}\left\{Ei\left[\frac{-r^2}{4\alpha(t-t_0)}\right] - Ei\left[\frac{-r^2}{4\alpha t}\right]\right\} \\ & + \frac{q'}{4\pi\lambda}\left\{Ei\left[\frac{-(r^2+4d^2)}{4\alpha(t-t_0)}\right] - Ei\left[\frac{-(r^2+4d^2)}{4\alpha t}\right]\right\} \quad t \geq t_0\end{aligned} \tag{2}$$

The ILS-ABC model includes two terms, the first term is the heating probe induced ΔT (equation (1)), and the second term is the virtual heating probe induced ΔT. In this study, the plane of heat and temperature probes are parallel to the soil-atmosphere interface (Fig. 1), so the distance between the virtual heating probe and the temperature probe is $\sqrt{r^2+4d^2}$.

COMSOL Simulations

We used the two-dimensional transient heat conduction module of COMSOL (COMSOL, Inc., Burlington, MA) to simulate the effects of wind with high v on DPHP measurements. The COMSOL simulations able us to study the effects of wind on simulated DPHP measurements without interferences from other factors. A rectangle with dimensions of 70 mm by 100 mm with zero initial temperature was used to model the DPHP system near the soil-atmosphere interface. The effects of wind with different v values was expressed by different values of heat transfer coefficient (h) of the upper boundary, and the other three boundary conditions were adiabatic boundary conditions as the default setting of COMSOL. We simplified the heating probe into a circle with a radius of 0.6 mm, and the temperature probe as a point. In order to reduce the number of elements in the COMSOL simulations, the epoxy filling and Delrin plug of the DPHP sensor were neglected, and physical properties of the subdomain were assumed to be constants (Liu et al., 2013b). Dry sand, unsaturated sand, and saturated sand were chosen as our three simulated soil samples, and we set t_0 =

15s, q' = 23 W m^{-1}, 23 W m^{-1} and 60 W m^{-1}, bulk density (ρ_b) = 1690 kg m^{-3}, 1850 kg m^{-3} and 2000 kg m^{-3}, volumetric water content (θ) = 0, 0.16 cm^3 cm^{-3} and 0. 36 cm^3 cm^{-3}, c = 750 J kg^{-1} K^{-1}, 1059 J kg^{-1} K^{-1} and 1347 J kg^{-1} K^{-1}, λ = 0.3 W m^{-1} K^{-1}, 1.83 W m^{-1} K^{-1} and 2.8 W m^{-1} K^{-1}, for the dry sand, unsaturated sand and saturated sand, respectively.

We further simplified the soil–atmosphere interface into a flat-plate, which was in the form of the upper boundary of the domain used in the COMSOL simulations. According to equation (3), the Reynolds numbers (Re) in our experiments were less than 1.31×10^5, so we considered wind to be laminar flow and used the heat transfer coefficient (h) to express the effects of wind. The values of Re and h were calculated as (Whitaker, 1972):

$$\mathrm{Re} = \frac{\rho_a \upsilon L}{\mu_a} \tag{3}$$

$$h = 0.664 \frac{\lambda_a}{L} \left(\frac{\rho_a \upsilon L}{\mu_a} \right)^{1/2} \left(\frac{\mu_a c_a}{\lambda_a} \right)^{1} \tag{4}$$

where L is the length of the flat-plate, and λ_a, ρ_a, μ_a, c_a are the thermal conductivity, density, dynamic viscosity, specific heat of air, respectively, and at 20° C, the property values are 0.03 W m^{-1} K^{-1}, 1.19 kg m^{-3}, 18.20 μ Pa s, 1.00 kJ kg^{-1} K^{-1}, respectively (Lemmon and Jacobsen, 2004).

Laboratory Experiments and Field Experiments

The sensor used in this study consisted of one heating probe and two temperature probes (Fig. 1). A heating wire (Nichrome A, 79-μm diam, 205 Ωm^{-1}, Pelican Wire Co., Naples, FL) was installed in the heating probe, and two thermistors 15 mm and 25 mm away from the sensor base, were installed in each temperature probe (Liu et al., 2013a). This temperature probe design is capable of determining probe spacing in situ, although we did not make the in situ determination. In addition, compared to the temperature probe with only one installed thermistor at mid-length, the two-thermistor DPHP probes that we used doubled the measured data sets, and thus minimized the error in fitted parameters. All three probes had a length of 40 mm and were constructed from stainless-steel tubing (Small Parts Inc., Miami Lakes, FL) with 1.27-mm-o.d. and 0.84-mm-i.d. Three probes with spacing of 6 mm were secured to a 30.0 mm thick and 25.0 mm diameter Delrin plug using epoxy.

Dry sand, which was oven-dried at 105° C for 24 hours, was used in this study, because the relatively large particles helped to ensure that the value of d remained constant during DPHP measurements. Fine soil was sensitive to wind erosion, and it was difficult to maintain a constant burial depth, so, we did not use fine soil. We also excluded unsaturated samples because evaporation led to heterogeneity of soil water content (Merz et al., 2016) which invalidated the homogeneous assumption of the DPHP method. In addition, the latent heat of water evaporation (Heitman et al., 2008) was equivalent to a heat sink across the

soil–atmosphere interface. This sink term made the heat conduction problem of DPHP more complicated and further deteriorated the process of parameter estimation by introducing extra error in both c and λ. Due to the complications with fine-textured soils and unsaturated soils we confined our measurements to dry sand.

If probe spacing is calibrated in an agar solution, the DPHP method tends to overestimate heat capacity of dry soil (Tarara and Ham, 1997; Ham and Benson, 2004). Thermal contact resistance between the probes and the surrounding soil is a possible reason for the overestimations (Basinger et al., 2003; Liu et al., 2012). To eliminate the influence of thermal contact resistance, we used the method of Mori et al. (2003) to calibrate the probe spacing in dry sand with known c = 751 J kg $^{-1}$ K $^{-1}$ (measured by differential scanning calorimeter, DSC, Q2000, TA, Instruments, New Castle, DE). After probe spacing calibrations, we installed the DPHP sensor in a 70 mm by 100 mm by 100 mm cubic acrylic container and positioned all probes parallel to the bottom of the container (Fig. 1). Dry sand was packed into the container by 10 mm layers with ρ_b = 1690 kg m^{-3} and d = 5 mm. The distance between the container bottom and the probes was large enough (65 mm > 2.37 by 6 mm) to avoid the impact of the bottom of the container on measurements (Campbell et al., 1991), but the effects of the soil–atmosphere interface or wind could effects the measurements.

In the laboratory experiments, we used an electric fan to produce wind, and v was measured at the edge of the container using a handheld anemometer. The wind direction and the heat pulse probes were perpendicular to each other (Fig. 1(a)). We took as our results the mean values of all four thermistor measured values. Five wind velocities were used (v = 0, 0.5, 1.5, 2.5, 3.5 m s^{-1}), and each velocity was repeated eight times. During the first 60s of each measurement, we measured the background room temperature and ensured that the fluctuations in 60s periods were within $\pm 0.02^{\circ}$ C.

Field experiments were performed at the China Agricultural University Research Station in Beijing, China from DOY 71 to 150 in 2019. We packed dry sand into the same container which was used in the laboratory experiments, and buried the container with the DPHP sensor into the field soil (Fig. 1(b)). We checked on the sand sample in the field daily. Data collected on rainy days were eliminated, because precipitation caused uneven soil water distributions, which violated the isotropic assumption of both ILS and ILS-ABC model. Whenever there was rain or any noticeable d variation caused by wind erosion, we discarded the sample and repacked dry sand into the container. Moisture absorbed from the atmosphere by dry sand in the field was negligible. The discarded samples, excluding the rainy day samples were oven dried to determine water content, which was less than 0.005 m^3 m^{-3}. An anemograph was positioned next to the container, and v was measured at 95 mm above the soil-atmosphere interface. Different from laboratory experiments and COMSOL simulations, wind velocity cannot be kept constant in the field, v values actually

represented the mean wind velocity during a 180s DPHP measurement. The anemograph could not accurately measure low wind speeds, $v \leq 0.22$ m s^{-1}, so, measurements at $v \leq 0.22$ m s^{-1} were eliminated from the analysis.

A CR3000 data logger (Campbell Scientific, Logan, UT), powered by a 12-V battery, controlled the electrical pulse current to the DPHP sensor and collected data. The heating strength was determined through the electrical current of a reference resistor (1-Ω, 1% tolerance; M0625, Vishay Resistors, Malvern, PA). The sampling frequency of the data logger was 1Hz and the heat pulse length was 15s. In field experiments, temperature and v signals were collected simultaneously, and the measurement interval was set as 10 minutes to capture adequate wind data.

Data Processing

Background temperature fluctuations occur in the field. Bristow et al. (1993) and Young et al. (2008) installed an additional reference temperature sensor to monitor background temperature fluctuations, but we, like other researchers, used the method of Jury and Bellantuoni (1976) (Abbreviated as MJB76) to account for ambient temperature fluctuations

(Heitman et al., 2010; Zhang et al., 2014; Peng et al., 2017). The linear de-trending method of MJB76 can be summarized as:

$$\Delta T(r,t) = T_i - T_f \quad (5)$$

where T_i were the datalogger collected temperature signals, T_f were the estimated background temperature evolution by a linear trend model. T_f can be obtained by using a linear regression of the measured temperature versus time curve before initiating a pulse of heat (Jury and Bellantuoni 1976):

$$T_f = at + \quad (6)$$

where a and b are two regression parameters. The MJB76 approach had some limitations, which we discuss in the section *"The limitations of MJB76 for field conditions"*. To minimize the limitations of MJB76, we used two methods to select data independently. Method A was used to remove background temperature trends that significantly deviated from a linear trend. We reconstructed the background temperature using the difference between measured DPHP temperature values and the ILS-ABC model predicted temperature values using the known values of λ_0, c_0 and d, and then used root mean square error (RMSE) between the linear trend (Jury and Bellantuoni, 1976) and the reconstructed background temperature curves to select data with RMSE < 0.3° C. Method B was used to remove large background temperature fluctuations. We directly eliminated data from 8:00 to 19:00 daily

to remove the effects of solar radiation, which caused drastic background temperature variations.

The built-in Findfit function of Wolfram Mathematica 11.3 (Wolfram Research, Inc., Champaign, IL) was used to obtain λ and c. Relative error was used to evaluate the effects of wind on DPHP measurements and was defined as:

$$100 \times \frac{m - m_0}{m_0} \qquad (7)$$

where m and m_0 were the measured (λ_m or c_m) or simulated (λ_s or c_s) and the actual (λ_0 or c_0) value of λ or c, respectively. In laboratory experiments and field experiments, the values of λ_0 (0.3 W m^{-1} K^{-1}) and c_0 (751 J kg^{-1} K^{-1}) were measured during probe spacing calibrations and DSC measurements, respectively. In COMSOL simulations, the values of λ_0 and c_0 were the physical property values we inputted in the subdomain setting.

RESULTS AND DISCUSSION

The Performance of the ILS And ILS-ABC Model

Our results (Fig. 2) showed that when the ILS-ABC model was used instead of the ILS model, relative errors in c of dry sand could be reduced significantly when d = 5 mm and $v \leq 3.5$ m s^{-1}. For example, when d = 5 mm and v = 1.5 m s^{-1}, the relative error in c was reduced to 4% from −11% by replacing the ILS model with the ILS-ABC model. Similar to the studies of Liu et al. (2013b) and Zhang et al. (2014), in which they reported on v = 0 m s^{-1},

accurate estimations of surface soil λ and c could be obtained through the ILS-ABC model. Relative errors in λ_m and c_m of dry sand showed that as v increased the accuracy of the DPHP method with the ILS model was improved, while the accuracy of the DPHP method with the ILS-ABC model decreased. For example, when the ILS model was used, the relative error was −22% in λ_m and −14% in c_m for v = 0 m s^{-1}, and it was reduced to −11% in λ_m and −8% in c_m for v = 3.5 m s^{-1}. The convection of air increased heat dissipation which caused the soil-atmosphere interface to deviate from the adiabatic boundary condition, and the DPHP system matched more closely to the assumption of the ILS model. This phenomenon also meant that if the wind velocity was large enough, the ILS model could perform better than the ILS-ABC model. We explored whether this conjecture was correct or not using COMSOL simulation results in the section "*Relative error due to different wind velocity (v) and burial depth (d)*". According to the results of Heya et al. (1982), for air, when the Reynold number was between 10^4 and 10^7 (in our experiment the Reynold number < 10^5), there was no influence of surface roughness (≥ 600 μm) on the local heat-transfer coefficient. So, the differences between the errors of sand and the errors of fine soil, that were caused by wind were undistinguishable. Therefore, the same conclusions drawn from the sand experiments remained unchanged for finer soil and coarser soils. However, we need to perform actual experiments in the future to test these conclusions. Fig. 2 also indicates that the effects of wind on λ and c differ. Effects of the property change at the soil-atmosphere interface were also reported by Liu et al (2013b). The different sensitivity

of the two parameters to the wind affected temperature versus time curves could be the reason, in part, for these differences.

Evaluation of COMSOL Simulations

The performance of COMSOL simulations was evaluated by comparing the simulated results to laboratory measured results on repacked dry sand. Fig. 2 shows relative errors in λ_m, c_m, λ_s and c_s for both the ILS and ILS-ABC models, indicating that simulated and measured results agreed well. For 0 m s^{-1} $\upsilon \leq$ 3.5 m s^{-1}, differences between λ_s and λ_m were within 3% and 4% for the ILS and ILS-ABC models, respectively. Likewise, differences between c_s and c_m were within 2% and 3% for the ILS and ILS-ABC models, respectively. Also, regression analysis showed that λ_m (or c_m) could be predicted by λ_s (or c_s), because the slopes of the regression equations were close to 1 with intercepts of 0 and $R^2 \geq 0.80$. Therefore, different h values (Equation. (4)) could accurately characterize the effects of wind for different υ. So, it is reasonable to use COMSOL simulations to further evaluate the effects of wind on DPHP measurements.

Relative Errors due to Different Wind Velocity (υ) and Burial Depth (d)

Fig. 3 shows how the relative errors changed with different values of d and υ in dry sand and saturated sand. Here, the value of h was varied from 0 to 55 W m^{-2} K^{-1} (which corresponded to $0 \leq \upsilon \leq$ 20 m s^{-1}), and the value of d was varied from 1 to 12 mm or to 15 mm (12 mm in Fig. 3 and 15 mm in Fig. 4). Results indicated that for dry sand, when $d \leq 6$

mm and $v \neq 0$ m s^{-1}, the effects of wind needed to be taken into account. The ILS-ABC model did not provide accurate estimations, and when d = 1 mm, the relative errors reached 28% in λ and 9% in c even if v = 0.5 m s^{-1}. However, for saturated sand, when 1 mm ≤ d ≤ 15 mm, the ILS-ABC model provided accurate λ estimations with relative errors ≤ 6% when $v \leq 1.5$ m s^{-1}, and relative errors in c were less than 3% when 0 m s^{-1} ≤ $v \leq 20$ m s^{-1}. In the following, we chose the results for d = 5 mm for varied v and v = 3.5 m s^{-1} for varied d to examine the effects of wind in detail.

For a fixed d value (5 mm) with varying v, the ILS model underestimated λ and c. The accuracy of the ILS model estimations increased as v increased. Relative errors in λ_s of dry sand ranged from −19% to −4%, and relative errors in c_s of dry sand ranged from −13% to −6% when v increased from 0 m s^{-1} to 20 m s^{-1} (Fig. 2(a)).When the DPHP sensor was installed near the soil-atmosphere interface, the use of the ILS model was equivalent to the assumption that $\lambda_a / \lambda = 1$. For v = 0 m s^{-1}, compared to soil, air had a smaller λ (≈ 0.03 W m^{-1} K^{-1}, Lemmon and Jacobsen, 2004). The poor thermal conduction in air resulted in heat accumulation at the soil-atmosphere interface, and caused underestimations in both λ and c. As v increased, the heat dissipating into the atmosphere accounted for an increasingly higher share, which was equivalent to the increased value of λ_a, which caused the ILS model assumptions to become suitable, and DPHP estimations with the ILS model became increasingly accurate. As for the ILS-ABC model, accurate estimations in c (the absolute values of relative error ≤ 1%) for saturated sand or overestimated λ and c of dry sand and

λ of saturated sand were likely to occur, and both the λ and c values increased as v increased. When v varied from 0 to 20 m s^{-1}, relative errors in λ varied from 7% to 31%, and relative errors in c varied from −2% to 6% for dry sand (Fig. 2(a)). That was due to the ILS-ABC model assumption that λ_a = 0 W m^{-1} K^{-1} or λ_a/λ = 0, which was a good approximation for v = 0 m s^{-1} (Liu et al., 2013b). But as v increased, contradictions emerged between the DPHP system and the ILS-ABC model assumption, and the soil-atmosphere interface gradually could not be well approximated as an adiabatic boundary.

For saturated sand, the variation of relative errors with increasing v had a similar trend as that for dry sand. Compared to the results of dry sand, relative errors were aggravated if the ILS model was used, while relative errors were reduced significantly if the ILS-ABC model was used (Fig. 2(a)). That was due to the fact that compared to dry sand, saturated sand had much larger thermal property values (de Vries, 1963; Abu-Hamdeh, 2003; Mengistu et al. 2017). Thus, compared to dry sand, it was more prone to the situation of $\lambda_a/\lambda \rightarrow 0$ for the whole change range of v, and the ILS-ABC model was more suitable for determining thermal properties of saturated sand.

Fig. 4 illustrated how the wind with v = 3.5 m s^{-1} (the maximum wind velocity generated in our laboratory) affected DPHP measurements for varied d values. In general, the trend was similar to the results of Liu et al (2013b) with v = 0. For dry sand, both the

ILS and ILS-ABC models gave poor estimations for both λ and c and had significant relative errors when $d \leq 4$ mm. It was worth noting that when $d \leq 4$ mm, if the ILS-ABC model was used, relative errors in λ were ≥ 27% and relative errors in c were ≥ 6%. Simulations by Liu et al. (2013b) showed that when $d \leq 4$ mm, the ILS-ABC model provided accurate estimations with the absolute values of relative errors ≤ 6%. The divergence between our results and those of Liu et al. (2013b) was clearly caused by wind, we deduced that, for dry sand with $d \leq 4$ mm, the effects of wind with v =3.5 m s^{-1} was non-negligible. Additionally, the ILS and ILS-ABC models gave similar predictions when $d \geq 8$ mm, indicating the effects of wind with v =3.5 m s^{-1} was negligible when $d \geq 8$ mm. For saturated sand, the ILS-ABC model provided accurate estimations of c (the absolute values of relative error ≤ 1%) when $d \geq 1$ mm, and accurate estimations of λ (the absolute values of relative error ≤ 3%) when $d \geq 9$ mm. If the ILS model was used for saturated sand, the relative errors in λ were significant (the absolute values of relative error ≥ 16%) until $d > 9$ mm. For unsaturated sand, the simulated results showed that the relative errors in either c or λ as a function of d displayed similar trends as the dry sand and the saturated sand. Meanwhile, the relative error for unsaturated sand was between the relative errors of the saturated sand and the dry sand. Compared to the dry sand, the difference between thermal diffusivity values of the unsaturated sample (ρ_b = 1850 kg m^{-3}, c = 1059 J kg^{-1} K^{-1}, λ = 1.83 W m^{-1} K^{-1}) and that of the saturated sand (ρ_b = 2000 kg m^{-3}, c = 1347 J kg^{-1} K^{-1}, λ = 2.8 W m^{-1} K^{-1}) was

roughly 10%, which resulted in a near overlapping of the errors of these two conditions (Fig. 4).

The Limitations of MJB76 for Field Conditions

Because fluctuations of relative errors in λ_m and c_m were very large during the daytime (Fig. 5), we speculated that the soil background temperature trends could not be well approximated by a simple linear relationship (Jury and Bellantuoni, 1976; Zhang et al., 2017) as the reason. In addition, we assumed that solar radiation was a major contributor to soil temperature fluctuations. To test these conjectures, we examined background temperature signals for various luminous intensities. As Fig. 6(a) indicates, the linear trend derived from the first 60s temperature signals collected before starting a heating pulse differ from the actual background temperature evolution data collected from the onset of heating to the end of the DPHP measurements (60s < t < 180s). For the temperature versus time curve in Fig. 6, at 180s, the difference between the extended linear trend and the actual background temperature variation curves was 2.5° C, and the root mean square error (RMSE) between the two curves was 0.99° C. For an infinite, homogeneous and isotropic medium with such background temperature fluctuations, MJB76 gave relative errors of −52% in λ and −31% in c. MJB76 only performed well for linear background temperature fluctuations. So, in our analysis, we excluded DPHP data with non-linear background temperature fluctuations (we used method A or B to guide data exclusions, see the section on *"Data processing"*). Fig. 6a

also indicates that extreme changes in background temperatures might be the result of sudden changes in solar radiation (luminous intensity in Fig. 6(c)). Further field investigations are needed to clarify the influence of solar radiation on background temperature evolution, especially during partly cloudy conditions.

Relative Errors due to v When d = 5 mm in the Field

Wind velocity measured by the anemograph was less than 2.7 m s^{-1}, which was consistent with the study of Smith et al. (1994), and velocities were less than 2.1 m s^{-1} after using method A or method B to select data for analysis. As Fig. 7 shows, method B results are more concentrated than method A results, Because for method B, DPHP measured data from 8 am to 7 pm are not analyzed. If the magnitude of background temperature fluctuations was correlated to solar radiation (Fig. 6), applying method A did not completely eliminate the solar radiation effect.

The raw data relative errors for method A and method B displayed large scatter, as was shown in Fig. 7. For a given v, the raw data relative error was larger than the COMSOL simulated errors in both λ and c (within 7%) when d = 5 mm and 0.22 m s^{-1} < v ≤ 2.1 m s^{-1}. The error associated with the field experiments may have originated from variations in d, the temperature dependence of λ and c (Liu and Si, 2010), the stochastic and chaotic characteristic of wind (Fig. 5(b)), non-homogeneous soil temperature distribution. Thus, the relative errors in λ and c on v were super positioned up on noisy signals.

To extract the effects of wind on DPHP measurements from the noisy raw data, we divided data presented in Fig. 7 into four groups: 0.22 m s^{-1} < v ≤ 0.5 m s^{-1}, 0.5 m s^{-1} < v ≤ 1.0 m s^{-1}, 1.0 m s^{-1} < v ≤ 1.5 m s^{-1} and 1.5 m s^{-1} < v ≤ 2.1 m s^{-1}. After grouping the data, the mean relative errors within each group and the corresponding mean v (0.36 m s^{-1}, 0.75 m s^{-1}, 1.25 m s^{-1} and 1.8 m s^{-1}) were determined. Fig. 7 indicates raw value differences between method A and B, but after grouping the data, the differences between method A and method B errors decreased remarkably. And the mean relative errors in each group were similar. For example, in the fourth group, the difference in the mean relative error in λ_{ILS} between methods A and B was 7%. In method B, daytime temperature data from 8 am to 7 pm were removed, so, there were no large temperature fluctuations and no large errors in λ and c. For method B, the analyzed sand sample temperature was lower than that of method A. Because large temperature meant large thermal expansion, thermal expansion for method B was smaller than for method A. Because the larger the thermal expansion, the larger the thermal stress, larger thermal stress resulted in good thermal contact (Liu et al., 2017) and larger thermal contact conductance. According to Liu et al (2012), poor thermal contact between soil particles and the DPHP probe reduced thermal contact conductance, which corresponded to underestimated λ values. The results of Liu et al (2012) could explain our findings in Fig. 7, i.e., the mean relative errors in λ of method B were smaller than those of method A in each of the four groups.

Fig. 7 also shows that relative error in each of the four groups is consistent with the corresponding relative errors in laboratory experiments and COMSOL simulations. For example, when v = 1.5 m s^{-1}, if the ILS-ABC model was used, relative errors in λ were 17% in laboratory experiments, 15% in COMSOL simulations and 15% in field experiments (after averaging in the fourth group: 1.5 m s^{-1} < v ≤ 2.1 m s^{-1}). Field experiments once again demonstrated that when the DPHP sensor was installed near the soil-atmosphere interface, the errors in DPHP measured λ and c were correlated with v. But when v was small (< 2.1 m s^{-1} in our field experiments) the major error origin of the DPHP method could be the dramatic background temperature fluctuations when the DPHP sensor was installed near the soil-atmosphere interface. In this paper, we only studied the effects of wind on DPHP measured thermal properties. The effects of wind on ground heat flux and dynamic soil water evaporation warrant future study.

CONCLUSIONS

When a DPHP sensor was installed near the soil-atmosphere interface, the effects of wind was related to v, d and soil thermal properties. COMSOL simulations showed that when d = 5 mm and 0 m s^{-1} ≤ v ≤ 20 m s^{-1}, the ILS model underestimated λ and c, and the accuracy of the ILS model increased as v increased. The ILS-ABC model provided accurate estimations of c for saturated sand, but the accuracy of the ILS-ABC model decreased as v increased. In laboratory experiments with d = 5 mm and v ≤ 3.5 m s^{-1}, for

dry sand the ILS-ABC model provided more accurate estimations in c than did the ILS model. For field measurements with $v \leq 2.7$ m s^{-1}, the ILS-ABC model always performed better than the ILS model. Many factors, especially diurnal background temperature fluctuations, resulted in highly noisy λ and c values. When the field measurement results were averaged within selected wind velocity intervals, they were similar to results obtained in laboratory experiments and COMSOL simulations.

REFERENCES

Abu-Hamdeh, N.H. 2003. Thermal properties of soils as affected by density and water content. Biosystems. Eng. 86(1): 97-102. doi: 10.1016/S1537-5110(03)00112-0

Basinger, J.M., G.J. Kluitenberg, J.M. Ham, J.M. Frank, P.L. Barnes, and M.B. Kirkham. 2003. Laboratory evaluation of the dual-probe heat-pulse method for measuring soil water content. Vadose Zone J. 2: 389- 399. doi: 10.2113/2.4.552

Bristow, K.L., G.S. Campbell, and K. Calissendorff. 1993. Test of a heat-pulse probe for measuring changes in soil water content. Soil Sci. Soc. Am. J. 57:930-934. doi:10.2136/sssaj1993.03615995005700040008x

Bristow, K.L., G.J. Kluitenberg and R. Horton. 1994. Measurement of soil thermal properties with a dual-probe heat-pulse technique. Soil Sci. Soc. Am. J. 58(5): 1288-1294. doi: 10.2136/sssaj1994.03615995005800050002x

Bristow, K.L., J.R. Bilskie, G.J. Kluitenberg and R. Horton. 1995. Comparison of techniques for extracting soil thermal-properties from dual-probe heat-pulse data. Soil Sci. 160(1): 1-7. doi: 10.1097/00010694-199507000-00001

Campbell, G.S., C. Calissendorff and J.H. Williams. 1991. Probe for measuring soil specific heat using a heat-pulse method. Soil Sci. Soc. Am. J. 55(1): 291-293. doi: 10.2136/sssaj1991.03615995005500010052x

Carslaw, H.S., and J.C. Jaeger. 1959. Conduction of heat in solid. Clarendon Press, Oxford.

Cosenza, P., R. Guerin and A. Tabbagh. 2003. Relationship between thermal conductivity and water content of soils using numerical modelling. Eur. J. Soil Sci. 54(3): 581-587. doi: 10.1046/j.1365-2389.2003.00539.x

Cobos, D.R. and J.M. Baker. 2003. In situ measurement of soil heat flux with the gradient method. Vadose Zone J. 2(4): 589-594. doi:10.2113/2.4.589.

de Vries, D.A. 1952. A nonstationary method for determining thermal conductivity of soil in situ. Soil Sci. 73:83-89. doi:10.1097/00010694195202000-00001

de Vries, D.A. 1963. Thermal properties of soils. In: Physics of plant environment, (ed. W.R. Van Wijk), pp. 210-235. North-Holland Publishing Corporation, Amsterdam.

Ham, J.M., and E.J. Benson. 2004. On the construction and calibration of dual-probe heat capacity sensors. Soil Sci. Soc. Am. J. 68:1185-1190. doi:10.2136/sssaj2004.1185.

Heya, N., Takeuchi, M., and Fujii, T. 1982. Influence of surface-roughness on free-convection heat-transfer from a horizontal cylinder. Chem. Eng. J. 23(2): 185-192. doi: 10.1016/0300-9467(82)80010-5.

He, H., M. Dyck, R. Horton, T. Ren, K. L. Bristow, J. Lv, and B. Si. 2018. Development and application of the heat pulse method for soil physical measurements. Rev. Geophys. 56(4): 567-620. doi:10.1029/2017RG000584.

Heitman, J.L., R. Horton, T.J. Sauer and T.M. DeSutter. 2008. Sensible heat observations reveal soil-water evaporation dynamics. J. Hydrometeorol. 9(1): 165-171. doi: 10.1175/2007JHM963.1

Heitman, J.L., Horton, R., Sauer, T.J., Ren, T.S. and Xiao, X. 2010. Latent heat in soil heat flux measurements. Agric. For. Meteorol. 150(7-8): 1147-1153. doi: 10.1016/j.agrformet.2010.04.017

Hopmans, J.W., J. Simunek and K.L. Bristow. 2002. Indirect estimation of soil thermal properties and water flux using heat pulse probe measurements: geometry and dispersion effects. Water Resour. Res. 38(1). doi: 10.1029/2000WR000071

Jury, W.A., and B. Bellantuoni. 1976. A background temperature correction for thermal conductivity probes. Soil Sci. Soc. Am. J. 40(4): 608-610. doi: 10.2136/sssaj1976.03615995004000040040x

Kettridge, N. and A. Baird. 2007. In situ measurements of the thermal properties of a northern peatland: Implications for peatland temperature models. J. Geophys. Res. Earth Surf. 112(F2). doi: 10.1029/2006JF000655

Kamai, T., G.J. Kluitenberg and J.W. Hopmans. 2015. A dual-probe heat-pulse sensor with rigid probes for improved soil water content measurement. Soil Sci. Soc. Am. J. 79(4): 1059-1072. doi: 10.2136/sssaj2015.01.0025

Lemmon, E.W., and Jacobsen, R.T. 2004. Viscosity and thermal conductivity equations for nitrogen, oxygen, argon, and air. Int. J. Thermophys. 25(1): 21-69. doi: 10.1023/B:IJOT.0000022327.04529.f3

Liu, G and B.C. Si. 2010. Errors in the heat pulse probe method: experimental and simulation analysis. Soil Sci. Soc. Am. J. 74(3):797-803. 2010. doi: 10.2136/sssaj2009.0116

Liu, G., Si, B.C., Jiang, A.X., Li, B.G., Ren, T.S. and Hu, K.L. 2012. Probe body and thermal contact conductivity affect error of heat pulse method based on infinite line source approximation. Soil Sci. Soc. Am. J. 76(2): 370-374. doi: 10.2136/sssaj2011.0228n

Liu, G., M.M. Wen, X.P. Chang, T.S. Ren, and R. Horton. 2013a. A self-calibrated dual probe heat pulse sensor for in situ calibrating the probe spacing. Soil Sci. Soc. Am. Jo. 77(2): 417-421. doi: 10.2136/sssaj2012.0434n

Liu, G., L.J. Zhao, M.M. Wen, X.P. Chang and K.L. Hu. 2013b. An adiabatic boundary condition solution for improved accuracy of heat-pulse measurement analysis near the soil-atmosphere interface. Soil Sci. Soc. Am. J. 77(2): 422-426. doi: 10.2136/sssaj2012.0187n

Liu, G., Yili Lu, M. Wen, Tusheng Ren and R. Horton, 2017. Advances in the heat-pulse technique: improvements in measuring soil thermal properties. Methods of Soil Analysis. 2(1): msa2015.0028.

Lu, S., Wang, H.S., Meng, P., Zhang, J.S., and X. Zhang. 2018. Determination of soil ground heat flux through heat pulse and plate methods: Effects of subsurface latent heat on surface energy balance closure. Agric. For. Meteorol. 260: 176-182. doi: 10.1016/j.agrformet.2018.06.008

Lu, Y.L., R. Horton and T. Ren. 2018. Simultaneous determination of soil bulk density and water content: a heat pulse-based method. Eur. J. Soil Sci. 69 (5): 947-952. doi: 10.1111/ejss.12690

Lu, Y.L., S. Lu, R. Horton and T.S. Ren. 2014. An empirical model for estimating soil thermal conductivity from texture, water content, and bulk density. Soil Sci. Soc. Am. J. 78(6): 1859-1868. doi: 10.2136/sssaj2014.05.0218

McCafferty, D.J., J.B. Moncrieff and I.R. Taylor. 1997. The effect of wind speed and wetting on thermal resistance of the barn owl (tyto alba). I: total heat loss, boundary layer and total resistance. J. Therm. Biol. 22(4-5): 253-264. doi: 10.1016/S0306-4565(97)00020-X

McVicar, T.R., Roderick, M.L., Donohue, R.J., Li, L.T., Van Niel, T.G. Thomas, A., Grieser, J., Jhajharia, D., Himri, Y., Mahowald, N.M., Mescherskaya, A.V., Kruger, A.C., Rehman, S., Dinpashoh, Y. 2012. Global review and synthesis of trends in observed terrestrial near-surface wind speeds: Implications for evaporation. J. Hydrol. 416: 182-205. doi: 10.1016/j.jhydrol.2011.10.024

Mengistu, A,G., L.D. van Rensburg and S.S.W. Mavimbela. 2017. The effect of soil water and temperature on thermal properties of two soils developed from aeolian sands in South Africa. Catena. 158: 184-193. doi: 10.1016/j.catena.2017.07.001

Merz, S., Pohlmeier, A., Balcom, BJ., Enjilela, R and Vereecken, H. 2016. Drying of a natural soil under evaporative conditions: a comparison of different magnetic resonance methods. Appl. Magn. Reson. 47(2): 121-138. doi: 10.1007/s00723-015-0736-6

Mori, Y., J. W. Hopmans, A. P. Mortensen, and G. J. Kluitenberg. 2003. Multi-functional heat pulse probe for the simultaneous measurement of soil water content, solute concentration, and heat transport parameters. Vadose Zone Journal 2 (4):561-71. doi:10.2136/vzj2003.5610

Philip, J.R. and G.J. Kluitenberg. 1999. Errors of dual thermal probes due to soil heterogeneity across a plane interface. Soil Sci. Soc. Am. J. 63(6): 1579-1585. doi: 10.2136/sssaj1999.6361579x

Poulsen, T.G., A. Furman and D. Liberzon. 2018. Effect of near-surface wind speed and gustiness on horizontal and vertical porous medium gas transport and gas exchange with the atmosphere. Eur. J. Soil Sci. 69(2): 279-289. doi:10.1111/ejss.12531.

Peng, X., Y. Wang, J. Heitman, T. Ochsner, R. Horton and T. Ren. 2017. Measurement of soil-surface heat flux with a multi-needle heat-pulse probe. Eur. J. Soil Sci. 68(3): 336-344. doi: 10.1111/ejss.12421

Redecker, K.R., A.J. Baird. and Y.A. Teh. 2015. Quantifying wind and pressure effects on trace gas fluxes across the soil-atmosphere interface. Biogeosciences. 12(24): 7423-7434. doi: 10.5194/bg-12-7423-2015

Ren, R.Q., Liu, G. Wen, M.M., Horton, R., Li, B.G. and Si, B.C. 2017. The effects of probe misalignment on sap flux density measurements and in situ probe spacing correction methods. Agric. For. Meteorol. 232: 176-185. doi: 10.1016/j.agrformet.2016.08.009

Smith, C.C., Lof, G. and R. Jones. 1994. Measurement and analysis of evaporation from in inactive outdoor swimming pool. Sol. Energy. 53(1): 3-7. doi: 10.1016/S0038-092X(94)90597-5

Sturm, M., Perovich, D.K. and Holmgren, J. 2002. Thermal conductivity and heat transfer through the snow on the ice of the Beaufort Sea. J. Geophys. Res.-Oceans. 107(C21). doi: 10.1029/2000JC000409

Tarara, J.M., and J.M. Ham. 1997. Measuring soil water content in the laboratory and field with dual-probe heat-capacity sensors. Agron. J. 89:535-542. doi: 10.2134/agronj1997.00021962008900040001x

Whitaker, S. 1972. Forced convection heat transfer correlations for flow in pipes, past flat plates, single cylinders, single spheres, and for flow in packed beds and tube bundles. Aiche J. 18(2): 361-371. doi: 10.1002/aic.690180219

Xiao, X., X. Zhang, T. Ren, R. Horton and J.L. Heitman. 2015. Thermal property measurement errors with heat pulse sensors positioned near a soil-air interface. Soil Sci. Soc. Am. J. 79(3): 766-771. doi: 10.2136/sssaj2014.12.0493n

Young, M. H., Campbell, G.S. and J. Yin. 2008. Correcting dual-probe heat-pulse readings for changes in ambient temperature. Vadose Zone J. 7(1): 22-30. doi: 10.2136/vzj2007.0015

Zhang, X., J. Heitman, R. Horton and T. Ren. 2014. Measuring near-surface soil thermal properties with the heat-pulse method: correction of ambient temperature and soil-air interface effects. Soil Sci. Soc. Am. J. 78(5): 1575-1583. doi: 10.2136/sssaj2014.01.0014

Zhang, X., T. Ren, J. Heitman, and R. Horton. 2017. Advances in heat-pulse methods: Measuring near-surface soil water content. Methods of Soil Analysis. 2(1): msa2015.0032. doi:10.2136/msa2015.0032

FIGURE CAPTIONS

Fig. 1 Side view of schematic diagram of (a) the device in laboratory experiments with d = 5 mm, five υ were used (i.e. υ = 0, 0.5, 1.5, 2.5, and 3.5 m s^{-1}); (b) top view of the device used in field experiments with d = 5 mm and υ was measured by an anemograph.

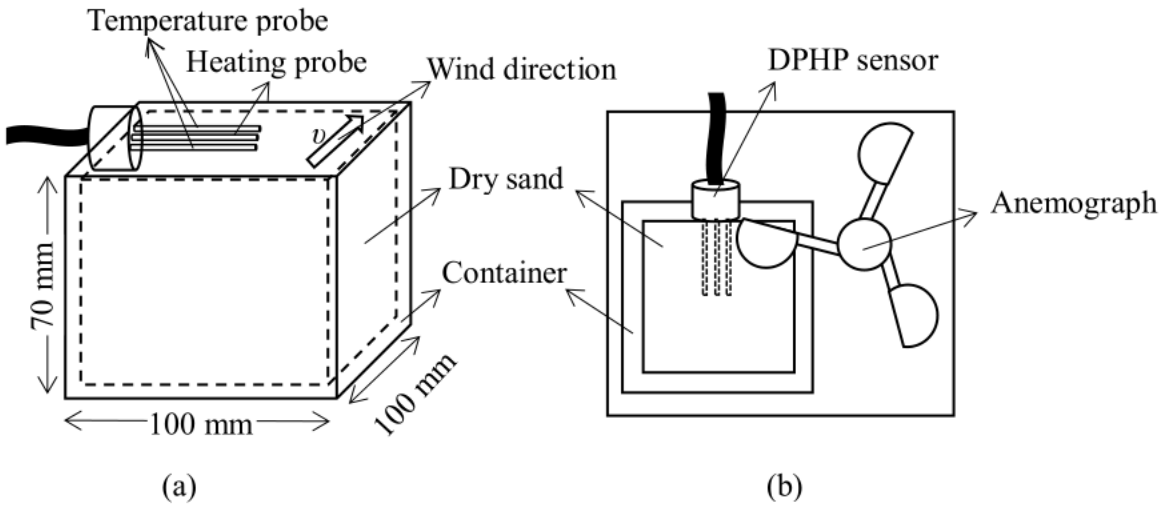

Fig. 2 (a) Relative errors in λ and c for probes in dry sand and saturated sand with d = 5 mm and varying v. The subscripts ILS and ILS-ABC mean that the DPHP temperature signals were processed by the ILS and ILS-ABC models, respectively. (b) The enlarged part of (a) within the frame.

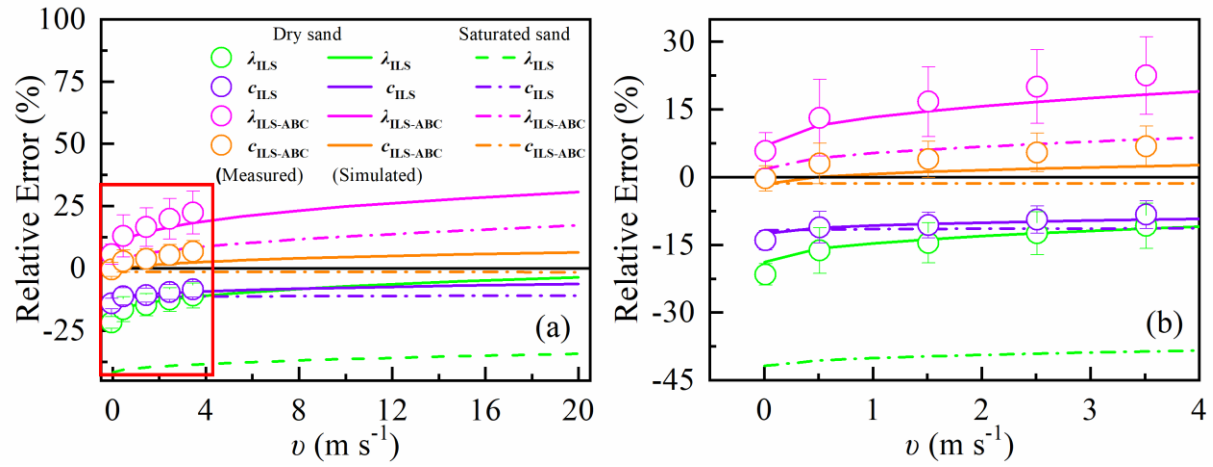

Fig. 3 Contour plots of the relative errors obtained by COMSOL simulations as functions of burial depth (d) and wind velocity (v) in dry sand and saturated sand. The subscripts ILS and ILS-ABC mean that the DPHP temperature signals were processed by the ILS and ILS-ABC models, respectively.

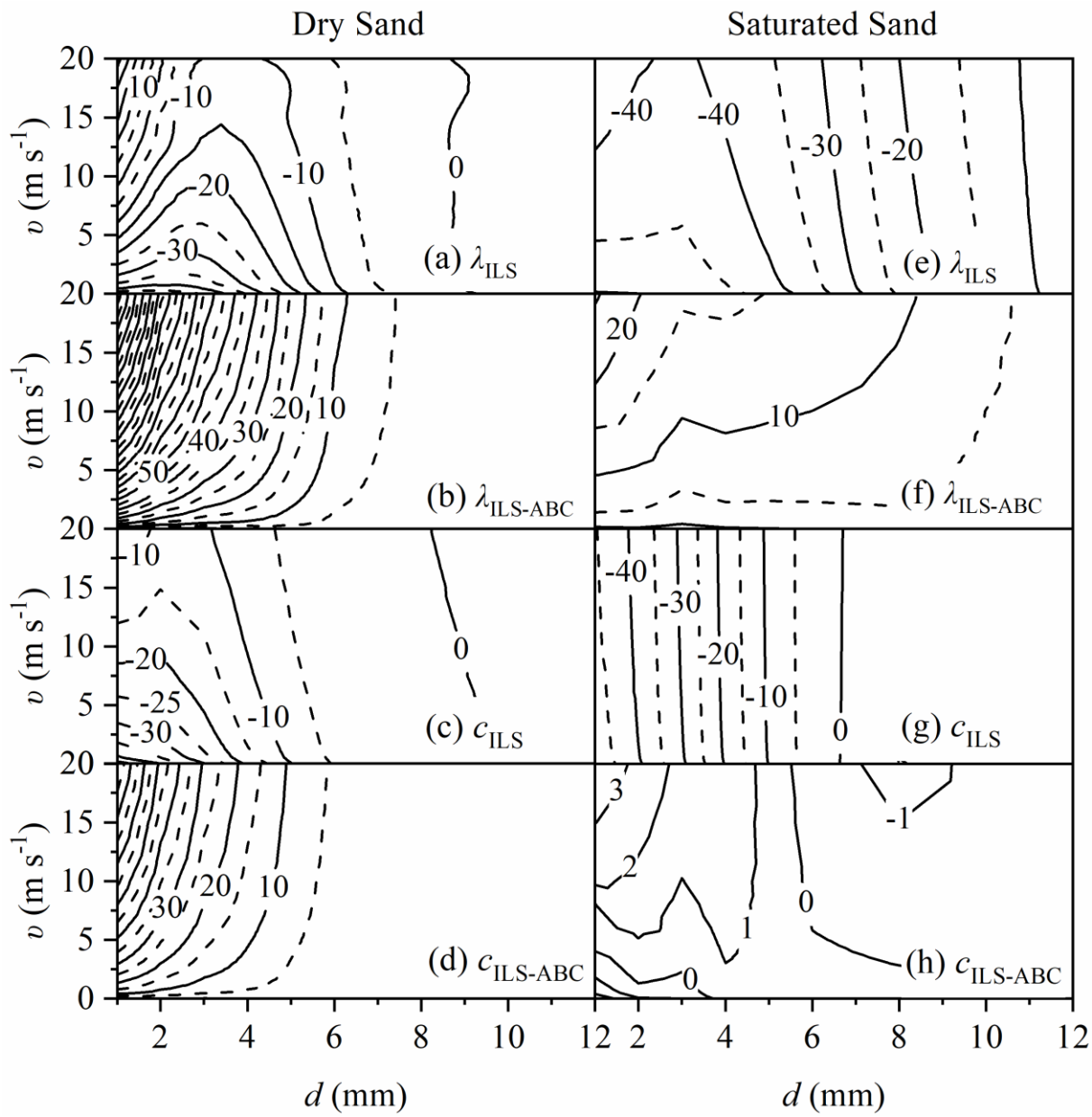

Fig. 4 COMSOL simulated relative errors in λ and c for probes in dry sand, unsaturated sand and saturated sand with v = 3.5 m s^{-1} and varying d. The subscripts ILS and ILS-ABC mean that the DPHP temperature signals were processed by the ILS and ILS-ABC models, respectively.

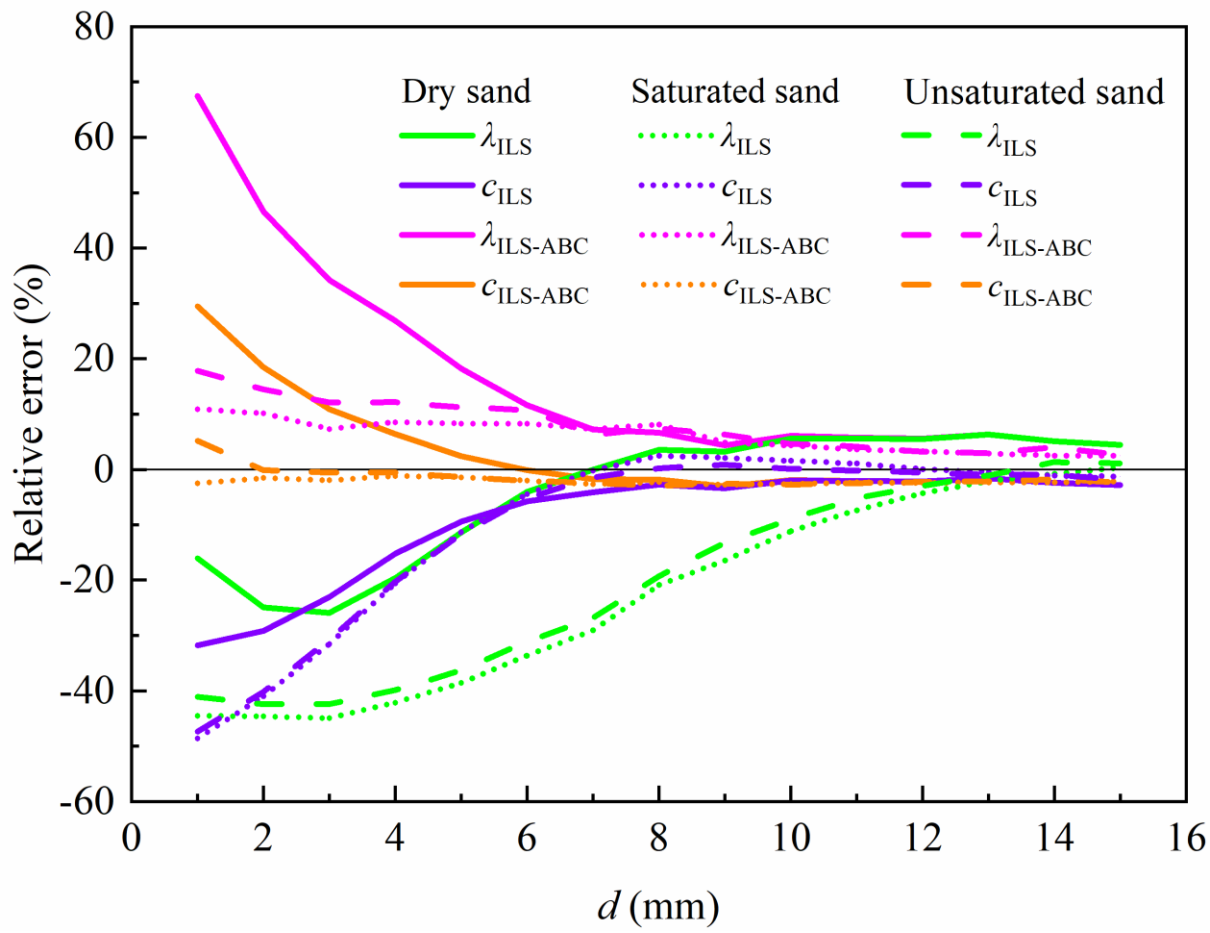

Fig. 5 Diurnal variation of relative errors in λ and c for probes in dry sand with d = 5 mm and varying v on DOY 76 in 2019. The subscripts ILS and ILS-ABC mean that the DPHP signals were processed by the ILS and ILS-ABC models, respectively. Squares were used to highlight the relatively large daytime error fluctuations in λ and c.

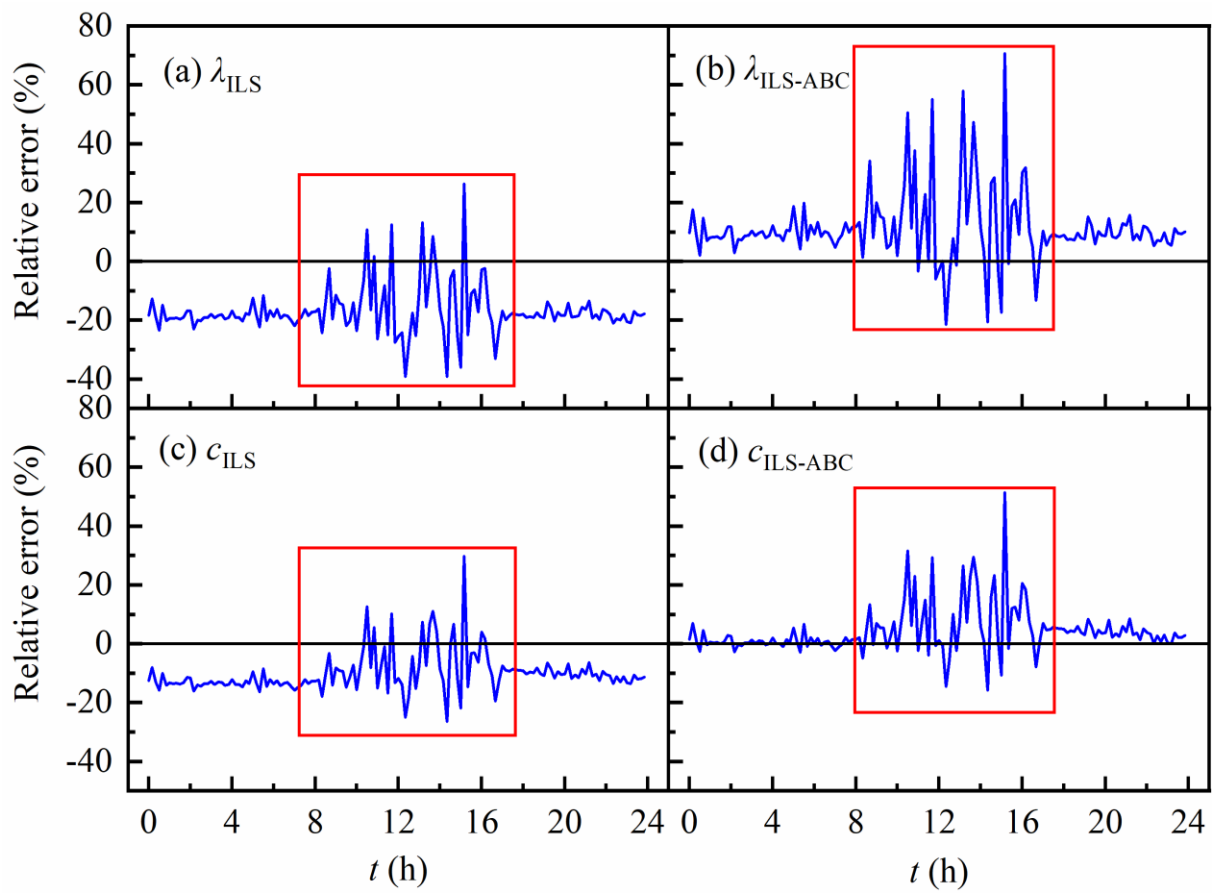

Fig. 6 Typical temperature (a), wind velocity (b) and luminous intensity (c) variations during a DPHP measurement (at 15:00 on DOY 139 in 2019).

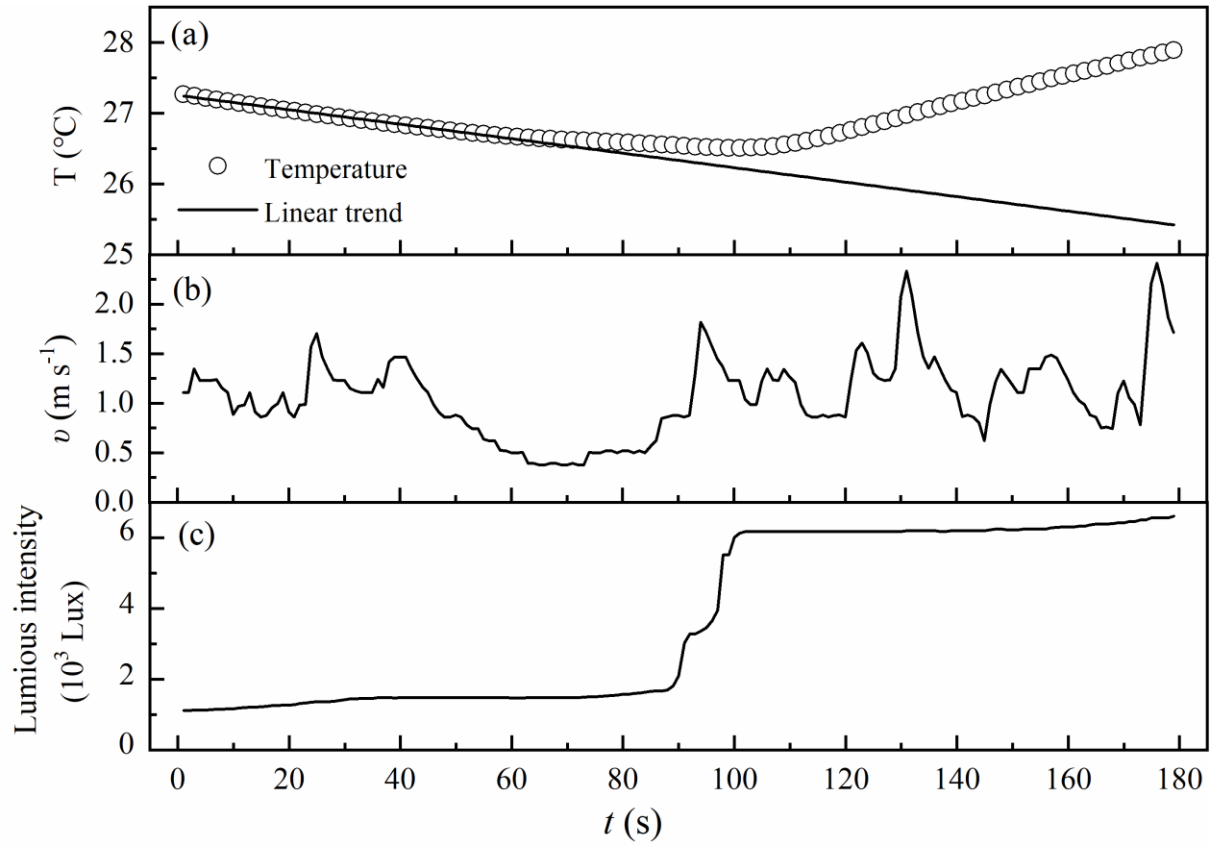

Fig. 7 Relative errors in λ and c for probes in dry sand with d = 5 mm and varying v in field experiments from DOY 71 to 102 in 2019. The black lines are relative errors derived from COMSOL simulations. The subscripts ILS and ILS-ABC mean that the DPHP signals are processed by the ILS and ILS-ABC models, respectively. Method A and method B indicate different data selecting methods. Mean values are presented for four groups (1st, 2nd, 3rd, and 4th) representing mean wind velocity values of 0.22 m s^{-1} < v ≤ 0.5 m s^{-1}, 0.5 m s^{-1} < v ≤ 1.0 m s^{-1}, 1.0 m s^{-1} < v ≤ 1.5 m s^{-1} and 1.5 m s^{-1} < v ≤ 2.1 m s^{-1}.